Sol-Gel Deposited Sb-Doped Tin Oxide Films

M. GUGLIELMI AND E. MENEGAZZO
Dip. Ing. Meccanica, S. Materiali, Università Padova, 35100 Padova, Italy

M. PAOLIZZI
Istituto Giordano SpA, Bellaria (RN), Italy

G. GASPARRO, D. GANZ, J. PÜTZ AND M.A. AEGERTER
Institut für Neue Materialien INM, Im Stadtwald, D-66123 Saarbrücken, Germany

L. HUBERT-PFALZGRAF
Laboratoire de Chimie Moléculaire (URA-CNRS), F-06108 Nice Cedex 2

C. PASCUAL AND A. DURÁN
Instituto de Ceramica y Vidrio (CSIC), 28500 Arganda del Rey (Madrid), Spain

H.X. WILLEMS AND M. VAN BOMMEL
Philips Research Laboratories, NL-5656 AA Eindhoven, The Netherlands

L. BÜTTGENBACH
Fa. E. Merck, ZGE, D-64293 Darmstadt, Germany

L. COSTA
Gel Design and Engineering (GDE), I-28100 Novara, Italy

Abstract. The structural, electrical and optical properties of single sol-gel derived antimony-doped tin oxide (ATO) films sintered at 550°C have been measured. The reproducibility of both the preparation and the characterization procedures have been tested by a round-robin test involving eight laboratories within a Concerted European Action (CEA) project. The resistivity measured as a function of Sb content has been obtained by electric and reflectance and transmission measurements. Their differences are discussed in terms of structural and grain boundary effects. An increase of Sb content results in a decrease of the crystallite size (7.0 to 5.4 nm) and a greater influence of the grain boundary.

Keywords: thin films, transparent conductors, Sb-doped tin oxide, optical properties, electrical properties

1. Introduction

Conductive and transparent coatings are essential in the development of optic and optoelectronic devices [1], displays [2], heat shields [2], solar energy applications [3], gas sensors [4], conductive paint coatings [5] and catalysts [6].

Sol-gel deposited ATO coatings have been described in several papers [7–15]. These previous studies have shown that their performances are worse than those

reported for coatings deposited by other deposition techniques [1, 14, 16] and depend on several parameters, such as the chemical composition of the solution (precursors, catalysts, amount of water, hydrolysis control reagents, concentration), layer thickness, heating procedure, and treatment atmosphere. The effect of these parameters is not completely understood and it is difficult to correlate the optical and electrical properties to the structural and chemical features of the material.

The aim of a project developed in the frame of a Concerted European Action [17] was to realize a round-robin test with seven laboratories (Università Padova (UP), Istituto Giordano (IG), Instituto de Ceramica y Vidrio (CSIC), Institut für Neue Materialien (INM), Philips Research Laboratories (PRL), Fa. E. Merck, Gel Design and Engineering (GDE)) with the aim to verify the reproducibility in the preparation and characterization of ATO coatings in terms of thickness, structural features (crystalline structure, average grain size), electrical and optical performances and to study the effect of antimony concentration. Some results are described in this paper, but a more complete description will be published elsewhere [18].

2. Experimental Procedures

Tin tert-butoxide ($Sn(OtBu)_4$) was used as precursor for tin oxide. Following the indications of a preliminary study on its alcoholysis and hydrolysis reaction [19] a sol (SOL 1) was prepared by dissolving $Sn(OtBu)_4$ in pure, anhydrous ethanol (EtOH) at a concentration $[Sn] = 0.33$ mol/l; then 1 equivalent of acetylacetone (acacH) was added and reacted for 2 h at room temperature; 2 moles of H_2O per mole of alkoxide were finally added.

Sb(III) ethoxide was used as precursor for antimony oxide. It was dissolved in pure, anhydrous ethanol at a concentration $[Sb] = 0.33$ mol/l (SOL 2).

The final sols were prepared by mixing SOL 1 and SOL 2 in the proportions to get a Sb/Sn molar ratio of 0.15 for the first series samples, and ranging from 0.02 to 0.15 for the second series. The concentration of this sol was about 50 g/l of oxides.

Doped tin oxide layers were deposited by spinning on Corning 7059 glass slides (in order to avoid problems related to alkali contamination) following a common procedure and using the same sources. For the first series, seven samples were produced at PRL, INM and UP. For the second series, the samples were produced at PRL and distributed for characterization.

Heat treatment was performed in air. Samples were dried at 80°C for 2 h, heated to 550°C at 5 K/min, left for 10 min at 550°C and then cooled in the furnace down to 350°C.

The thickness of the films was measured by surface profilometry. The films were analyzed at UP by X-ray diffraction using a diffractometer equipped with a glancing-incidence X-ray optics. The average crystallite size was calculated from the Scherrer equation after fitting the experimental profiles.

A detailed optical study was performed on the second series of samples at IG where the spectral transmittance and reflectance were measured at normal incidence, in the range 0.25–2.5 μm. The optical constants n and k, thickness and resistivity ρ_{opt}, were obtained from these measurements assuming a homogeneous, isotropic layer texture and a Drude-Lorentz dispersion relationship.

Electrical resistivity measurements (ρ) were performed at room temperature by 4-point technique (INM, Merck, UP and PRL) and 4 point ac impedance spectroscopy (CSIS).

The details on the equipment and procedures used for characterization will be reported elsewhere [18].

3. Results and Discussion

X-ray diffraction was performed on all the samples. Tin oxide was present in its tetragonal form (cassiterite). No significant differences among the samples produced by different laboratories were found.

Crystallite size was calculated from the broadening of the (110) and (101) lines. A systematic decrease, from 7.0 to 5.4 nm, was observed with increasing antimony oxide content.

Table 1 presents the data of thickness for the first series of samples (15 at% Sb). There are significant

Table 1. Thickness d (nm) for samples of the first series measured by profilometer (*) and calculated from optical results (+).

	Source		
Measurement	UP	PRL	INM
UP*	73	75	78
INM*	63	67	75
IG+	63	71	79

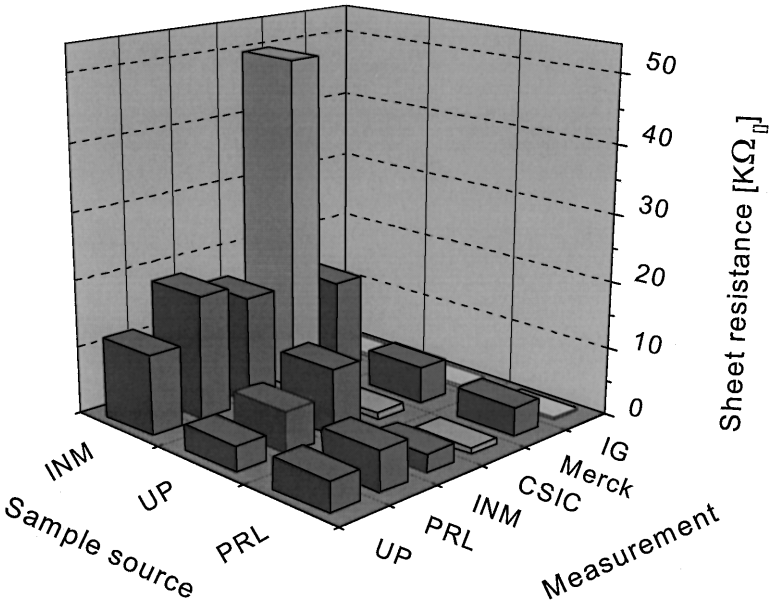

Figure 1. Sheet resistance for samples of the first series (15 at% Sb) measured by 4-point technique at UP, PRL, INM, Merck, 4-point ac impedance spectroscopy at CSIC and calculated from optical measurement at IG.

deviations in the measured values not only between the different source of preparation, but also from the measuring laboratories. The values calculated from optical data are close to those measured by profilometer.

Figure 1 shows the data of the sheet resistance ($R_\square$) for the same series. The electrical values measured by different laboratories on the samples coming from the same source show a large distribution, the differences being larger than those coming from the preparation of the samples in the various laboratories. These differences are certainly due to the conditions under which the measurements were performed and the time elapsed between the fabrication and the measurement. The ac measurements performed at CSIC under a dry atmosphere and controlled temperature showed, in fact, an instability of the electrical properties. For example, the resistance of the INM sample was found to decrease from 50 to 14 k$\Omega_\square$ after heating to 100°C. With PRL and UP samples the instability was observed also at room temperature: the PRL sample increased its resistance from 0.87 to 1.05 k$\Omega_\square$ after two days in the measurement cell and to 1.7 k$\Omega_\square$ after heating at 100°C and cooling down to room temperature. Therefore, the experimental conditions (humidity, atmosphere, temperature, geometry, etc.) should be defined more precisely. The values calculated from the optical data for samples prepared in 3 laboratories are in good agreement but are at least one order of magnitude smaller than the electrically measured ones.

The samples containing different Sb contents (second series) were analyzed in the same way and the results are summarized in Tables 2 and 3.

Table 2. Thickness d, mobility μ, carrier density n, resistivity ρ, and sheet resistance $R_\square$, measured at INM by the van der Pauw/Hall method (second series).

Sb content (at%)	t (nm)	ρ (10^{-3} Ωcm)	μ (cm^2/Vs)	n (cm^{-3})	$R_\square$ (kΩ/□)
2	68.8	38,7	1.1	1.5×10^{20}	5.8
4	73.2	33,1	0.9	2.2×10^{20}	4.5
6	69.2	26,7	0.8	3.0×10^{20}	3.8
8	69.4	20,2	1.0	3.1×10^{20}	2.9
10	70.0	21,0	0.8	3.7×10^{20}	3.0
15	69.3	19,0	0.8	4.5×10^{20}	2.7

Table 3. Thickness d, resistivity ρ_{opt}, and sheet resistance $R_\square$ calculated at IG from optical measurements (second series).

Sb content (at%)	d (nm)	ρ_{opt} (10^{-3} Ωcm)	$R_\square$ (kΩ/□)
2	70	11.1	1.57
4	70	4.4	0.62
6	69	2.8	0.40
8	70	2.6	0.37
10	69	2.4	0.35
15	69	2.3	0.34

The thickness determined by the two different methods are again in good agreement. As the Sb concentration increases by a factor 7, the already low values of the mobility slightly decrease and the carrier density increases by a factor 3 and seems to saturate for higher concentrations. As a consequence the resistivity decreases only by a factor 2 (Table 2).

On the other hand, the values of ρ_{opt} (Table 3) calculated from the optical spectra are again an order of magnitude lower than the ones measured electrically, except for the sample with 2 at% Sb. It should be remembered that the optical data have been taken at short wavelengths ($<2,5\ \mu$m) which act as a microscopic probe from which mainly the intra-grain resistivity is extracted. On the other hand, the electric determinations probe macroscopic areas (≈ 1 cm^2) averaging the response over a large number of grains. These are intersected by grain boundaries which introduce an effective electron scattering reducing the electron mobility and thus increasing the resistivity. The difference between the values obtained by these two methods should thus come essentially from the influence of the grain boundaries. This trend, evident in Fig. 2, seems to indicate that grain boundary scattering becomes more important for high Sb contents possibly due to the smaller grain size and/or a segregation of Sb(III) at grain boundaries [20]. Thus, the decrease in mobility cannot be completely attributed to ionized impurities scattering from the dopant. The index of refraction of the samples with different Sb content was evaluated at $\lambda = 500$ nm. It increased from 1.65 to 1.75 with increasing Sb content possibly indicating a denser packing of the crystallites [18].

4. Conclusions

The first series of experiments have shown that the preparation of the coatings has to be described more precisely in order to get a sufficient reproducibility. This involves the chemical procedures, the coating process, and the subsequent heat treatment. Furthermore, the electrical measurements and the storage of the samples have to be carried out under standardized conditions (humidity, temperature) to obtain comparable results.

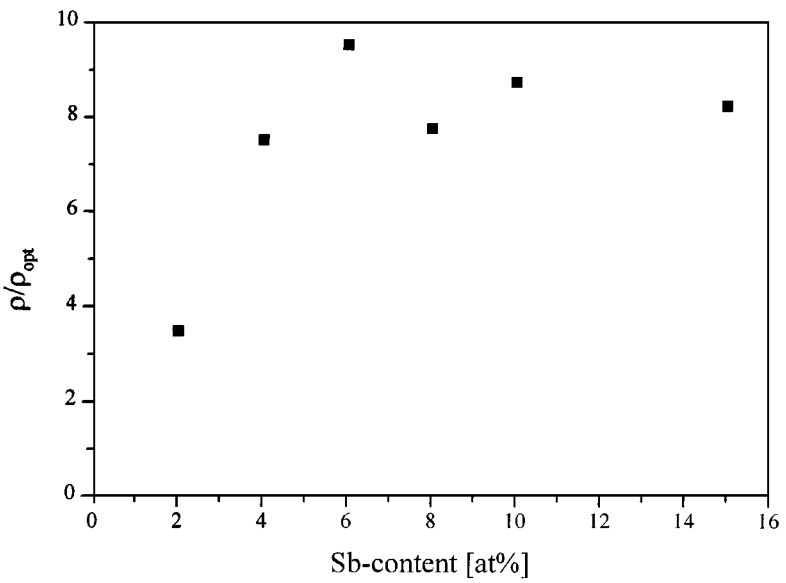

Figure 2. Ratio between resistivity values obtained from electrical measurements, ρ, and calculated from optical data, ρ_{opt}.

The combination of electrical and optical measurements proved to be a powerful means in the investigation of micro structural properties of the samples. In the second series it could be shown that the influence of the grain boundaries increase with increasing Sb content which was attributed to a reduction in crystallite size in combination with a possible segregation of Sb(III) on the surface of the crystallites.

Acknowledgments

This work was done in the frame of the Concerted European Action "Sol-Gel Processing for Advanced Industrial Material Technologies." The authors thank the European Commission of the European Community for their financial support.

References

1. K.L. Chopra, S. Major, and D.K. Pandya, Thin Solid Films **102**, 1 (1983).
2. C.G. Granquist, Thin Solid Films **193/194**, 730 (1990).
3. C.M. Lampert, Solar Energy Mater. **6**, 1 (1981).
4. W. Göpel and K.-D. Schierbaum, Sens. Actuators B **26/27**, 1 (1995).
5. Yoshizumi and K. Wakabayashi, Plastics Eng. 61 (1987).
6. Ono, T. Yamanaka, Y. Kubokawa, M. Komiyama, and J. Catal. **109**, 423 (1988).
7. C.J.R. Gonzales-Oliver and I. Kato, J. Non-Cryst. Solids **82**, 400 (1986).
8. G. Gowda and D. Nguyen, Thin Solid Films **136**, L39 (1986).
9. Y. Takahashi and Y. Wada, J. Electrochem. Soc. **137**, 267 (1990).
10. J.C. Giuntini, W. Granier, J.V. Zanchetta, and A. Taha, J. Mater. Sci. Lett. **9**, 1383 (1990).
11. B. Orel, U. Lavrencic-Stangar, Z. Crnjak-Orel, P. Bukovec, and M. Kosec, J. Non-Cryst. Solids **167**, 272 (1994).
12. J.P. Chatelon, C. Terrier, E. Bernstein, R. Berjoan, and J.A. Roger, Thin Solid Films **247**, 162 (1994).
13. S.-S. Park, H.X. Zheng, J.D. Mackenzie, Mater. Lett. **22**, 175 (1995).
14. C. Terrier, J.P. Chatelon, R. Berjoan, J.A. Roger, Thin Solid Films **263**, 37 (1995).
15. P. Olivi, E.C. Pereira, E. Longo, T.A. Varella, and L.O. de S. Bulhões, J. Electrochem., Soc. **140**, L81 (1993).
16. E. Shanti, V. Dutta, A. Banerjee, and K.L. Chopra, J. Appl. Phys. **51**, 6243 (1980).
17. Concerted European Action on "Sol-Gel Processing for Advanced Industrial Material Technologies."
18. M. Guglielmi, E. Menegazzo, M. Paolizzi, G. Gasparro, D. Ganz, J. Pütz, M.A. Aegerter, L. Hubert-Pfalzgraf, C. Pascual, A. Durán, H.X. Willems, M. van Bommel, L. Büttgenbach, and L. Costa, to be published.
19. S. Gaign and L.G. Hubert-Pfalzgraf, to be published.
20. D. Bélanger, J.P. Dodelet, B.A. Lombos, and J.I. Dickson, J. Electrochem. Soc. **132**, 1398 (1985).